The 11th International Conference on Geometry and Graphics, 1-5 August, 2004, Guangzhou, China

ON JACK PHILLIP'S SPATIAL INVOLUTE GEARING

Hellmuth STACHEL
Vienna University of Technology, Vienna, AUSTRIA

ABSTRACT This is a geometric approach to spatial involute gearing which has recently been developed by Jack Phillips (2003). After recalling Phillips' fundamental theorems and other properties, some geometric questions around this interesting type of gearing are discussed.
Keywords: Spatial gearing, involute gearing, helical involute

1 PRELIMINARIES

In the series of International Conferences on Geometry and Graphics there had been several papers dealing with spatial gearing, e.g. Podkorutov et al. (1998 and 2002), Andrei et al. (2002) or Brailov (1998).

The function of a gear set is to transmit a rotary motion of the input wheel Σ_1 about the axis p_{10} with angular velocity ω_{10} to the output wheel Σ_2 rotating about p_{20} with ω_{20} in a uniform way, i.e., with a constant *transmission ratio*

$$i := \omega_{20}/\omega_{10} = \text{const}. \qquad (1)$$

According to the relative position of the gear axes p_{10} and p_{20} we distinguish the following types:

a) Planar gearing (*spur gears*) for parallel axes p_{10}, p_{20},
b) spherical gearing (*bevel gears*) for intersecting axes p_{10}, p_{20}, and
c) spatial gearing (*hyperboloidal gears*) for skew axes p_{10}, p_{20}, in particular *worm gears* for orthogonal p_{10}, p_{20}.

1.1 Planar gearing

In the case of parallel axes p_{10}, p_{20} we confine us to a perpendicular plane where two systems Σ_1, Σ_2 are rotating against Σ_0 about centers 10, 20 with velocities ω_{10}, ω_{20}, respectively. Two curves $c_1 \subset \Sigma_1$ and $c_2 \subset \Sigma_2$ are *conjugate* profiles when they are in permanent contact during the transmission, i.e., (c_2, c_1) is a pair of enveloping curves under the relative motion Σ_2/Σ_1. Due to a standard theorem from plane kinematics (see, e.g., Wunderlich (1970) or Husty et al. (1997)) the common normal at the point *E* of contact must pass through the pole 12 of this relative motion. Due to the planar Three-Pole-Theorem this point 12 divides the segment 01 02 at the constant ratio *i* and is therefore fixed in the frame link Σ_0. We summarize:

Theorem 1 (Fundamental law of planar gearing):
The profiles $c_1 \subset \Sigma_1$ and $c_2 \subset \Sigma_2$ are conjugate if and only if the common normal e (= *meshing normal*) *at the point E of contact* (= *meshing point*) *passes through the relative pole* 12.

Due to L. Euler (1765) planar *involute gearing* (cf. e.g. Wunderlich (1970)) is characterized by the condition that with respect to Σ_0 *all meshing normals e are coincident*. This implies

(i) The profiles are *involutes* of the base circles.
(ii) For constant driving velocity ω_{10} the point of contact *E* runs relative to Σ_0 with constant velocity along *e*.
(iii) The transmitting force has a fixed line of action.
(iv) The transmission ratio *i* depends only on the dimension of the curves c_2, c_1 and not on their relative position. Therefore this planar gearing remains *independent of errors upon assembly*.

1.2 Basics of spatial kinematics

There is a tight connection between spatial kinematics and the geometry of lines in the Euclidean 3-space $\mathbb{E}^3$.
Therefore we start with recalling the use of appropriate line coordinates:

Any oriented line (*spear*) $g = \mathbf{a} + \mathbb{R}\mathbf{g}$ can be uniquely represented by the pair of vectors $(\mathbf{g}, \hat{\mathbf{g}})$, the *direction vector* $\mathbf{g}$ and the *momentum vector* $\hat{\mathbf{g}}$, with

$$\mathbf{g} \cdot \mathbf{g} = 1 \quad \text{and} \quad \hat{\mathbf{g}} := \mathbf{a} \times \mathbf{g}.$$

It is convenient to combine this pair to a *dual vector*

$$\underline{\mathbf{g}} := \mathbf{g} + \varepsilon \hat{\mathbf{g}},$$

where the dual unit ε obeys the rule $\varepsilon^2 = 0$. We extend the usual dot product of vectors to dual vectors and notice

$$\underline{\mathbf{g}} \cdot \underline{\mathbf{g}} = \mathbf{g}.\hat{\mathbf{g}} + 2\mathbf{g}.\hat{\mathbf{g}} = 1 + \varepsilon 0 = 1.$$

Hence we call $\underline{\mathbf{g}}$ a *dual unit vector*.
The dot product of dual vectors is defined by

$$\underline{\mathbf{g}} \cdot \underline{\mathbf{h}} = \mathbf{g}.\mathbf{h} + \varepsilon(\hat{\mathbf{g}}.\mathbf{h} + \mathbf{g}.\hat{\mathbf{h}}).$$

In the case of dual unit vectors this product has the following geometric meaning:

$$\underline{\mathbf{g}} \cdot \underline{\mathbf{h}} = \underline{\cos}\,\underline{\varphi} = \cos\varphi - \varepsilon\hat{\varphi}\sin\varphi \qquad (2)$$

where $\underline{\varphi} = \varphi + \varepsilon\hat{\varphi}$ is the *dual angle* (see Fig. 1) between the corresponding lines *g* und *h*, i.e., with $\varphi = \sphericalangle\, gh$ and $\hat{\varphi}$ as shortest distance (cf. Pottmann, Wallner (2001), p. 155 ff).

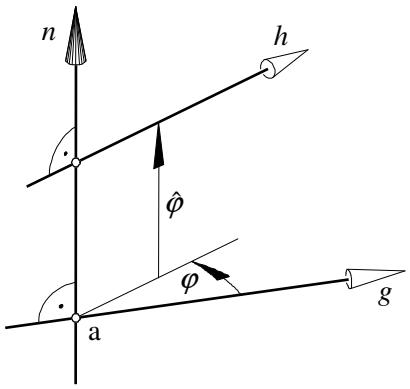

Figure 1: Two spears g, h enclosing the dual angle $\underline{\varphi} = \varphi + \varepsilon\hat{\varphi}$.

The components φ and $\hat{\varphi}$ of $\underline{\varphi}$ are signed according to any chosen orientation of the common perpendicular n. When the orientation of n is reversed then φ and $\hat{\varphi}$ change their sign. When the orientation either of g or of h is reversed then φ has to be replaced by $\varphi + \pi \pmod{2\pi}$.

There is also a geometric interpretation for non-normalized dual vectors: At any moment a spatial motion Σ_i/Σ_j assigns to the point $X \in \Sigma_i$ (coordinate vector $\mathbf{x}$) the *velocity vector*

$$ {}_X\mathbf{v}_{ij} = \hat{\mathbf{q}}_{ij} + (\mathbf{q}_{ij} \times \mathbf{x}) \tag{3}$$

relative to Σ_j. We combine the pair $(\mathbf{q}_{ij}, \hat{\mathbf{q}}_{ij})$ again to a dual vector $\underline{\mathbf{q}}_{ij}$. This vector can always be expressed as a multiple of a unit vector, i.e.,

$$\begin{aligned} \underline{\mathbf{q}}_{ij} &:= \mathbf{q}_{ij} + \varepsilon\hat{\mathbf{q}}_{ij} = \\ &= (\omega_{ij} + \varepsilon\hat{\omega}_{ij})(\mathbf{p}_{ij} + \varepsilon\hat{\mathbf{p}}_{ij}) = \underline{\omega}_{ij}\underline{\mathbf{p}}_{ij} \end{aligned}$$

with $\underline{\mathbf{p}}_{ij} \cdot \underline{\mathbf{p}}_{ij} = 1$. It turns out that ${}_X\mathbf{v}_{ij}$ coincides with the velocity vector of X under a helical motion (= *instantaneous screw motion*) about the *instantaneous axis* (ISA) with dual unit vector $\underline{\mathbf{p}}_{ij}$. The dual factor $\underline{\omega}_{ij}$ is a compound of the angular velocity ω_{ij} and the translatory velocity $\hat{\omega}_{ij}$ of this helical motion. $\underline{\mathbf{q}}_{ij}$ is called the *instantaneous screw*. In this sense, spears are the screws of rotations with angular velocity 1.

For each instantaneous motion (screw $\underline{\mathbf{q}}_{ij}$) the *path normals* n constitute a *linear line complex*, the (= *complex of normals*) as the dual unit vector $\underline{\mathbf{n}} = \mathbf{n} + \varepsilon\hat{\mathbf{n}}$ of any normal n obeys the equation

$$\hat{\mathbf{q}}_{ij} \,.\mathbf{n} + \mathbf{q}_{ij} \,.\hat{\mathbf{n}} = 0 \quad (\Leftrightarrow \underline{\mathbf{q}}_{ij} \cdot \underline{\mathbf{n}} \in \mathbb{R}). \tag{5}$$

This results from ${}_X\mathbf{v}_{ij} \,.\mathbf{n} = 0$ and $\hat{\mathbf{n}} = \mathbf{x} \times \mathbf{n}$. By (2) it is equivalent to

$$(\omega_{ij} + \varepsilon\hat{\omega}_{ij})\underline{\cos}\,\underline{\alpha} \in \mathbb{R} \text{ i.e. } \frac{\hat{\omega}_{ij}}{\omega_{ij}} = \hat{\alpha}\tan\alpha. \tag{6}$$

with $\underline{\alpha}$ denoting the dual angle between p_{ij} and any orientation of n.

The spatial Three-Pole-Theorem states (cf. Husty et al. (1997) or Stachel (2000)): *If for three given systems* Σ_0, Σ_1, Σ_2 *the dual vectors* $\underline{\mathbf{q}}_{10}$, $\underline{\mathbf{q}}_{20}$ *are the instantaneous screws of* Σ_1/Σ_0, Σ_2/Σ_0, *resp., then*

$$\underline{\mathbf{q}}_{21} = \underline{\mathbf{q}}_{20} - \underline{\mathbf{q}}_{10} \tag{7}$$

is the instantaneous screw of the relative motion Σ_2/Σ_1.

As a consequence, if a line n which intersects the ISAs p_{10} of Σ_1/Σ_0 and p_{20} of Σ_2/Σ_0 orthogonally, then it does the same with the axis p_{21} of Σ_2/Σ_1, provided $\omega_{21} \neq 0$.

For given skew axes p_{10}, p_{20}, but arbitrary dual velocities $\underline{\omega}_{10}$, $\underline{\omega}_{20}$ the axes p_{21} of the relative motions Σ_2/Σ_1 constitute a *cylindroid* or *Plücker conoid* (see, e.g., Pottmann, Wallner (2001), p. 181). Fig. 2 gives an impression of the cylindroid by showing some generators 'between' p_{10} and p_{20}.

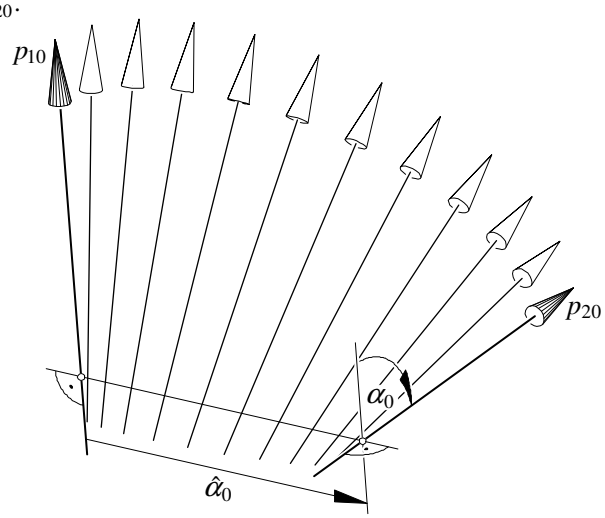

Figure 2: Generators of the cylindroid spanned by the screws $\mathbf{p}_{10}$ and $\mathbf{p}_{20}$.

For each ratio $\omega_{20}/\omega_{10} \neq 0, \infty$ the polodes Π_1, Π_2 of the relative motion Σ_2/Σ_1 are one-sheet hyperboloids of revolution which are in contact along p_{21} and have axes p_{10}, p_{20}, respectively. The common normal lines of Π_1 and Π_2 at the points of p_{21} intersect both, p_{10} and p_{20}, and constitute an orthogonal hyperbolic paraboloid.
We summarize:

Lemma 1 *The generators* p_{21} *of the cylindroid are characterized as those straight lines in space where a line contact can take place between one-sheet hyperboloids of revolution* Π_1, Π_2 *with mutually skew axes* p_{10}, p_{20}.

These hyperboloids are the spatial equivalents for *root and addendum circles* from planar gearing. They were used at the gearing displayed in Fig. 6.

1.3 Basics of spatial gearing

Let the systems Σ_1, Σ_2 rotate against Σ_0 about the fixed axes p_{10}, p_{20} with constant angular velocities ω_{10}, ω_{20}, respectively.

Then the instantaneous screw of the relative motion Σ_2/Σ_1 is constant in Σ_0, too.

It reads

$$\underline{\mathbf{q}}_{21} = \omega_{20}\underline{\mathbf{p}}_{20} - \omega_{10}\underline{\mathbf{p}}_{10} \quad \text{for} \quad \omega_{10}, \omega_{20} \in \mathbb{R}. \tag{8}$$

When two surfaces $\Phi_1 \subset \Sigma_1$ and $\Phi_2 \subset \Sigma_2$ are *conjugate* tooth flanks for a uniform transmission, then Φ_1 contacts Φ_2 permanently under the relative motion Σ_2/Σ_1.

In analogy to the planar case we obtain

Theorem 2 (Fundamental law of spatial gearing)
The tooth flanks $\Phi_1 \in \Sigma_1$ and $\Phi_2 \in \Sigma_2$ are conjugate if and only if at each point E of contact the contact normal e is included in the complex of normals of the relative motion Σ_2/Σ_1.

Due to (5) the dual unit vector $\underline{\mathbf{e}}$ of any meshing normal e obeys the equation of the linear line complex

$$\underline{\mathbf{q}}_{21} \cdot \underline{\mathbf{e}} = \omega_{20}(\underline{\mathbf{p}}_{20} \cdot \underline{\mathbf{e}}) - \omega_{10}(\underline{\mathbf{p}}_{10} \cdot \underline{\mathbf{e}}) \in \mathbb{R}.$$

Hence (2) implies for the dual angles $\underline{\alpha}_1$, $\underline{\alpha}_2$ between e and p_{10} and p_{20}, resp., (see Fig. 3, compare Phillips (2003), p. 46, Fig. 2.02)

$$\omega_{20}\hat{\alpha}_2 \sin\alpha_2 - \omega_{10}\hat{\alpha}_1 \sin\alpha_1 = 0$$

and therefore

$$i = \frac{\omega_{20}}{\omega_{10}} = \frac{\hat{\alpha}_1 \sin\alpha_1}{\hat{\alpha}_2 \sin\alpha_2}. \tag{9}$$

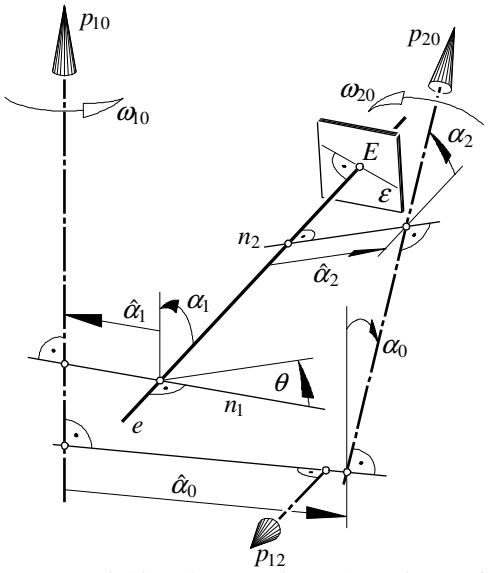

Figure 3: Spatial involute gearing: The point E of contact traces a fixed contact normal e.

2 SPATIAL INVOLUTE GEARING

Spatial involute gearing is characterized in analogy to the planar case as follows (cf. Phillips (2003)): *All contact normals e are coincident in* Σ_0 – and skew to p_{10} and p_{20}.[1] We exclude also perpendicularity between e and one of the axes.

According to (9) a constant contact normal e implies already a constant transmission ratio i.

[1] Note that in general this gearing offers *single point contact* only.

2.1 Slip tracks

First we focus on the paths of the meshing point E relative to the wheels Σ_1, Σ_2. These paths are called *slip tracks* c_1, c_2: Σ_1/Σ_0 is a rotation about p_{10}, and with respect to Σ_0 point E is placed on the fixed line e. Therefore – conversely – the slip track c_1 is located on the *one-sheet hyperboloid* Ψ_1 *of revolution* through e with axis p_{10}.[2]

On the other hand, the slip track c_1 is located on the tooth flank Φ_1, and for each posture of Φ_1 line $e \subset \Sigma_0$ is orthogonal to the tangent plane ε at the instantaneous point of contact (see Fig. 3).

Therefore the line tangent to the slip track c_1 is orthogonal to e. This gives the result:

Lemma 2 *The path c_1 of E relative to Σ_1 is an orthogonal trajectory of the e-regulus on the one-sheet hyperboloid Ψ_1 through e with axis p_{10}.*

We use a cartesian coordinate system[3] with the z-axis at p_{10} and the x-axis along the common perpendicular n_1 between p_{10} and e (see Fig. 3). Then the plane $z = 0$ contains the throat circle of the hyperboloid Ψ_1.

$$\Psi_1(u,v) = A(u) \cdot e(v) \text{ with}$$

$$A(u) = \begin{pmatrix} \cos u & -\sin u & 0 \\ \sin u & \cos u & 0 \\ 0 & 0 & 1 \end{pmatrix}, \; e(v) = \begin{pmatrix} \hat{\alpha}_1 \\ -v\sin\alpha_1 \\ v\cos\alpha_1 \end{pmatrix}$$

is a parametrization of Ψ_1 in matrix form and based on the parametrization $e(v)$ of the line e.
The curve $c_1(t) = \Psi_1[u(t), v(t)]$ intersects the v-lines orthogonally if

$$\left[\frac{dA}{du} \cdot e(v)\dot{u} + A(u) \cdot \frac{de}{dv}\dot{v}\right]^{\mathrm{T}} \cdot A(u) \cdot \frac{de}{dv} = 0.$$

This is equivalent to the differential equation

$$-\hat{\alpha}_1 \sin\alpha_1 \dot{u} + \dot{v} = 0.$$

Hence the slip track c_1 which starts in the plane $z = 0$ on the x-axis can be parametrized as

$$c_1(u) = A(u) \cdot e(\hat{\alpha}_1 \sin\alpha_i u) \tag{10}$$

or

$$c_1(u) = \hat{\alpha}_1 \begin{pmatrix} \cos u \\ \sin u \\ 0 \end{pmatrix} + \hat{\alpha}_1 u \sin^2\alpha_1 \begin{pmatrix} \sin u \\ -\cos u \\ \cot\alpha_1 \end{pmatrix}. \tag{11}$$

We obtain all other slip tracks on Ψ_1 by rotation about p_{10}. In order to describe the 'absolute motion' of the point E of contact, i.e., its motion with respect to Σ_0, we superimpose the rotation of the hyperboloid Ψ_1 about p_{10} with angular velocity ω_{10} with the movement of E along c_1 by setting $u = -\omega_{10}t$. Thus we obtain the path $e(-\omega_{10}\hat{\alpha}_1 \sin\alpha_1 t)$.

[2] As line e is different from the relative axis p_{21}, this one-sheet hyperboloid of revolution Ψ_1 differs from the polodes Π_1 mentioned in Lemma 1.

[3] A more geometric approach for this fact can be found in Stachel (2004).

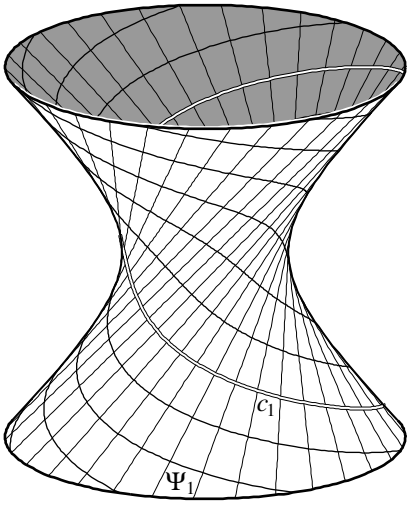

Figure 4: Slip tracks c_1 as orthogonal trajectories on the one-sheet hyperboloid Ψ_1 ($\hat{\alpha}_1 \sin\alpha_1 < 0$).

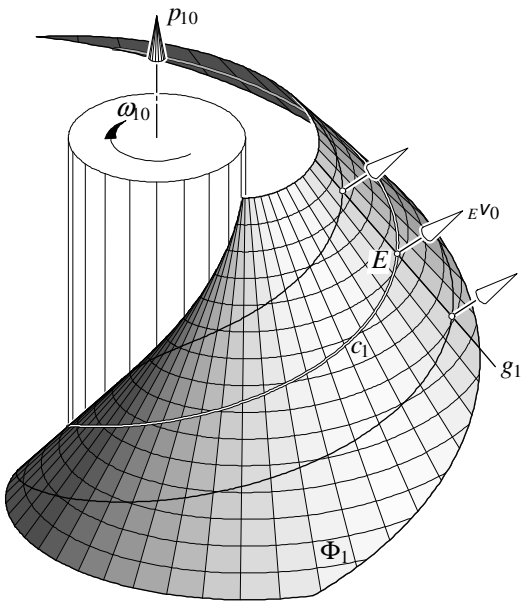

Figure 5: The tooth flank Ψ_1 (helical involute) with the slip track c_1 of point $E \in g_1$ ($\hat{\alpha}_1 \sin\alpha_1 > 0$).

This proves that E traces line e with the constant velocity vector

$$ {}_E\mathbf{v}_0 = -\omega_{10}\hat{\alpha}_1 \sin\alpha_1 \begin{pmatrix} 0 \\ -\sin\alpha_1 \\ \cos\alpha_1 \end{pmatrix}. \tag{12} $$

2.2 The tooth flanks

The simplest tooth flank for single point contact is the envelope Φ_1 of the plane ε of contact in Σ_1. By (12) this plane ε through E and perpendicular to e is translated along e and simultaneously rotated about p_{10}. Therefore Φ_1 it is a *helical involute* (see Fig. 5), the developable swept by tangent lines of a helix.

The parametrization in (11) can be rewritten as

$$ c_1(u) = \hat{\alpha}_1 \begin{pmatrix} \cos t \\ \sin t \\ t\tan\alpha_1 \end{pmatrix} - \hat{\alpha}_1 t \sin^2\alpha_1 \begin{pmatrix} -\sin t \\ \cos t \\ \tan\alpha_1 \end{pmatrix} \tag{13} $$

thus showing c_1 as a curve on Φ_1.

The first term on the right hand side parametrizes the edge of regression of Φ_1. The second term has the direction of tangent lines, the generators $g_1 \subset \Phi_1$.

Lemma 3 *The slip track c_1 is located on a helical involute Φ_1 with the pitch $\hat{\alpha}_1 \tan\alpha_1$. At each point $E \in c_1$ there is an orthogonal intersection between Φ_1 and the one-sheet hyperboloid Ψ_1 of Lemma* 2.

Different slip tracks on Φ_1 arise from each other by helical motions about p_{10} with pitch $\hat{\alpha}_1 \tan\alpha_1$.

We summarize:

Theorem 3 (Phillips' 1st Fundamental Theorem)
The helical involutes Ψ_1, Ψ_2 are conjugate tooth flanks with point contact for a spatial gearing where all meshing normals coincide with a line e fixed in Σ_0.

2.3 Two helical involutes in contact

The following theorem completes the confirmation that the advantages (ii)–(iv) of planar involute gearing as listed above are still true for spatial involute gearing:

Theorem 4 (Phillips' 2nd Fundamental Theorem)
If two given helical involutes Φ_1, Φ_2 are placed in mutual contact at point E and if their axes are kept fixed in this position, then Φ_1 and Φ_2 serve as tooth flanks for uniform transmission whether the axes are parallel, intersecting or skew. According to (9) *the transmission ratio i depends only on Φ_1 and Φ_2 and not on their relative position. Therefore this spatial gearing remains independent of errors upon assembly.*

Proof: When the two flanks Φ_1, Φ_2 rotate with constant angular velocities ω_{10}, ω_{20} about their axes p_{10}, p_{20} and point E runs relatively along the slip tracks with appropriate velocities, then with respect to Σ_0 point E traces e with the velocities

$$ -\omega_{10}\hat{\alpha}_1 \sin\alpha_1 \quad \text{and} \quad -\omega_{20}\hat{\alpha}_2 \sin\alpha_2 , $$

respectively, due to (12). By (9) these velocities are equal at any moment. Hence the initial contact between Φ_1 and Φ_2 at E is preserved under simultaneous rotations with transmission ratio i. □

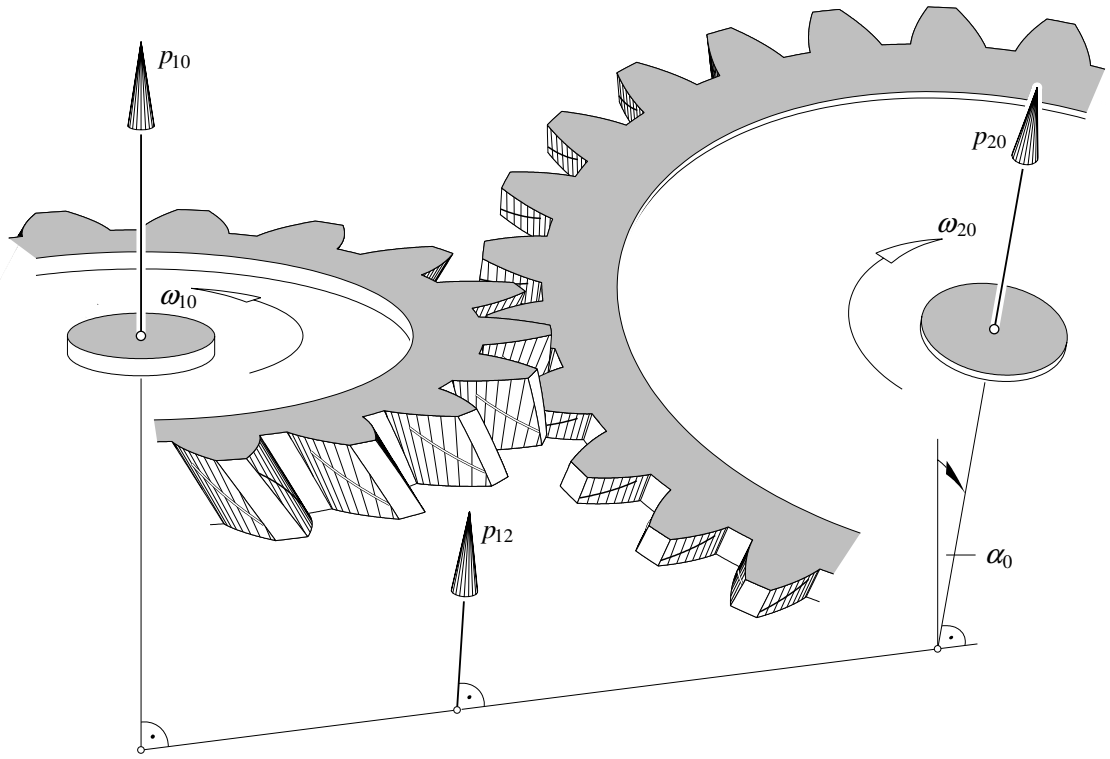

Figure 6: Spatial involute gearing together with the effective slip tracks on the flanks. List of dimensions: Transmission ratio $i = -2/3$, numbers of teeth: $z_1 = 18$, $z_2 = 27$; contact ratio 1.095; dual angle between p_{10} and p_{20} : $\alpha_0 = 21.35°$, $\hat{\alpha}_0 = 117.01$; dual angles between p_{i0} and the fixed contact normal e: $\alpha_1 = -60.0°$, $\hat{\alpha}_1 = 45.0$, $\alpha_2 = 76.98°$, $\hat{\alpha}_2 = 60.0$, and (compare Fig. 3) angle $\theta = 14.0°$.

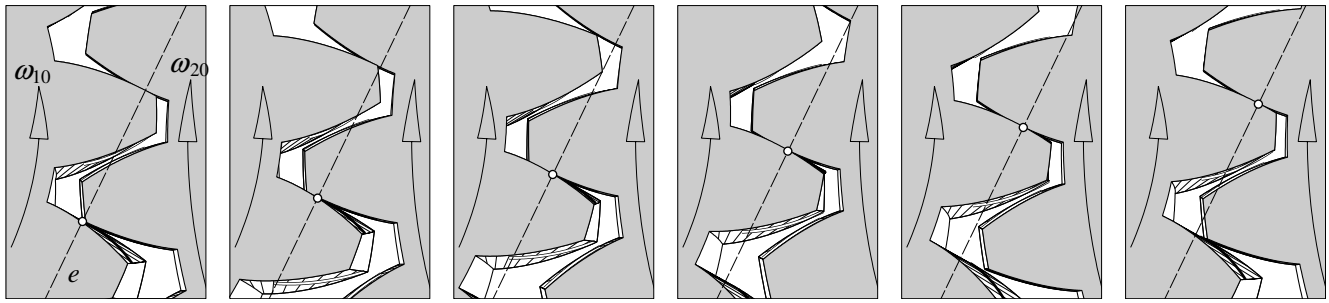

Figure 7: Different postures of meshing involute teeth for inspecting the backlash. e is the line of contact. Interval of the input angle $\Delta\varphi_{10} = 3.6°$, interval of the output angle $\Delta\varphi_{20} = -2.4°$.

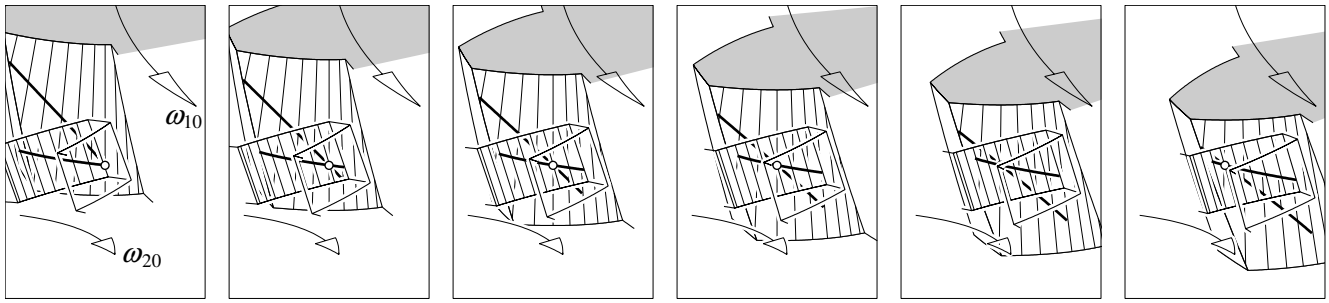

Figure 8: Different postures of meshing involute gear flanks together with the effective slip tracks, seen in direction of the contact normal e. The second wheel is displayed as a wireframe.

2.4 Involute gear flanks with line contact

Suppose there is any pair of flanks Φ_1, Φ_2 with permanent line contact while each point E of contact traces a straight line e in Σ_0.
Then the line g of contact generates in Σ_0 a ruled surface Γ while g remains an orthogonal trajectory of the generators.
Due to a standard theorem of Gauss any two orthogonal trajectories intersect all generators of Γ in segments of equal length. Therefore all points $E \in g \subset \Sigma_i$ must have the same absolute velocity $\|{}_E\mathbf{v}_0\|$ by (12), i.e., the dual angles $\underline{\nu}_i$ between surface normals n of Φ_i along g and the axis p_{i0} obey

$$\hat{\nu}_1 \sin \nu_1 = i\hat{\nu}_2 \sin \hat{\nu}_2 = c = \text{const.} \neq 0. \qquad (14)$$

This defines a (nonlinear) congruence of lines.
Conversely, with the arguments used in the proof of Theorem 4 we can confirm that these equations are sufficient for continuing line contact between Φ_1 and Φ_2.

Theorem 5
Φ_1, Φ_2 are flanks for involute gears with permanent contact along a curve g if and only if g is an orthogonal trajectory of a ruled surface Γ with generators included in the line congruence (14). *The flanks Φ_i are swept by slip tracks passing through the points $E \in g$.*
Particular examples of such flanks are the helical involutes mentioned in Theorem 3. Their generators are the lines of contact; the ruled surface Γ is a plane parallel to both axes p_{10} and p_{20} (cf. Stachel (2004)).

This particular example arises when the congruence (14) contains a line n which is located in a plane Γ parallel to p_{10} and p_{20}. Then all lines parallel to n and included in Γ obey (14), too.
Orthogonal trajectories of this pencil of parallel lines are generators of helical involutes Φ_1 and Φ_2 as mentioned in Lemma 3. In Fig. 5 a generator $g_1 \subset \Phi_1$ is depicted together with equal velocity vectors ${}_E\mathbf{v}_0$ at different points $E \in g_1$.

3 REFERENCES

Andrei, L., Andrei, G., Mereuta E., 2002, "Simulation of the curved face width spur gear generation and mesh using the solid modeling method", Proc. 10th ICGG, vol. 1, 245–248.

Brailov, A.Yu., 1998, "The Exclusion Method of Interference in Conjugated Helicoids", Proc. 8th ICECGDG Austin, vol. 2, 443–445.

Husty, M., Karger, A., Sachs, H., Steinhilper, W., 1997, "Kinematik und Robotik", Springer-Verlag, BerlinHeidelberg.

Phillips, J., 2003, "General Spatial Involute Gearing", Springer Verlag, New York.

Podkorutov, A.N., Malcev, D.V., 1998, „The geometry modelling of conjugate curved surfaces, excluding interference, scientific basic", 8th ICECGDG Austin, vol. 2, 446–449.

Podkorutov, A.N., Pavlyshko, A.V., Podkorytov, V.A., 2002, "Design of high-efficiency fair manyways wormy mills". Proc. 10th ICGG, vol. 1, 211–213.

Pottmann, H., Wallner, J., 2001, "Computational Line Geometry", Springer Verlag, Berlin, Heidelberg.

Stachel, H., 2000, "Instantaneous spatial kinematics and the invariants of the axodes". Proc. Ball 2000 Symposium, Cambridge, no. 23.

Stachel, H., 2004, "On Spatial Involute Gearing".TU Wien, Geometry Preprint No. **119**.

Wunderlich, W., 1970, "Ebene Kinematik", Bibliographisches Institut, Mannheim.

ABOUT THE AUTHORS

Hellmuth Stachel, Ph.D, is Professor of Geometry at the Institute of Discrete Mathematics and Geometry, Vienna University of Technology, and editor in chief of the "Journal for Geometry and Graphics". His research interests are in Higher Geometry, Kinematics and Computer Graphics.
He can be reached by e-mail: stachel@dmg.tuwien.ac.at, by fax: (+431)-58801-11399, or through the postal address:
Institut für Diskrete Mathematik und Geometrie / Technische Universität Wien / Wiedner Hauptstr. 8-10/104 /
A 1040 Wien / Austria, Europe.